Electronic Supplementary Information (ESI)

Conflux of tunable Rashba effect and piezoelectricity in flexible magnesium monochalogenide monolayers for next-generation spintronic devices

Manish Kumar Mohanta[†], Anu Arora[†] and Abir De Sarkar[*]

Institute of Nano Science and Technology, Knowledge City, Sector 81, Manauli, Mohali, Punjab-140306, India

*E-mail: abir@inst.ac.in; abirdesarkar@gmail.com

[†] Both the authors contributed equally

Born-Huang stability criteria[1];

$$C_{11} > |C_{12}|,\ C_{22} > 0,\ C_{66} > 0,\ C_{11}C_{22} - C_{12}^2 > 0 \quad \text{(S1)}$$

Young's modulus: $Y = (C_{11}C_{22} - C_{12}C_{21})/C_{22}$ (S2)

Poisson ratio: $v = \frac{C_{12}}{C_{22}}$ (S3)

Shear modulus: $G_{xy} = C_{66} = (C_{11} - C_{12})/2$ (S4)

Lang *et al*. formalism;

$$\mu_x = \frac{e\hbar^3\left(\frac{5C_{11}+3C_{22}}{8}\right)}{k_B T (m_x)^{\frac{3}{2}}(m_y)^{\frac{1}{2}}\left(\frac{9E_{1x}^2+7E_{1x}E_{1y}+4E_{1y}^2}{20}\right)} \times 10^4 \mathrm{cm^2V^{-1}s^{-1}} \quad \text{(S5)}$$

where $\hbar$, k_B and T is the electronic charge, reduced Planck's constant, Boltzmann constant, and temperature (300 K) respectively. $m_{x/y}$ are the effective masses of charge carriers along high symmetry direction and calculated by using the relation $m = \hbar^2[\partial^2 E(k)/\partial k^2]^{-1}$. The deformation potential $E_{1x/1y}$ is calculated from the slope of the linear fit of the variation in CBM and VBM with infinitesimal uniaxial lattice strain, as given in Fig. S2 and C_{ij} are 2D elastic stiffness constants tabulated in Table-4.

Mode Gr*ü*neisen parameter: It can be calculated directly from a change in phonon frequency with respect to volume dilation as given by the following eqn. S6

$$\gamma_i(q) = -\frac{d[\ln \omega_\lambda(q,V)]}{d[\ln V]} \quad \text{(S6)}$$

The volume of the unit cell is changed by applying infinitesimal small biaxial strain of ±0.005%. Then, the force constants have been obtained and the γ is evaluated.

Relaxation time approximation and Iterative solution to Boltzmann transport equation (BTE): In equilibrium, the distribution function of phonons is given by:

$$n^0_{q_v}(\omega, T) = \frac{1}{e^{\hbar\omega_q/\kappa_B T}-1} \quad \text{(S7)}$$

where q_v denotes a phonon with wave vector.

The distribution function can be expressed as a sum of the equilibrium term and a term representing the departure from the equilibrium[2];

$$n_q = n^0_q + \Delta n_q \quad \text{(S8)}$$

The relaxation time approximation assumes that the q at which a phonon relaxes does not depend on the equilibrium situation of the phonons colliding with it. In three phonon collision process; $n_{q'} = n^0_{q'}$ and $n_{q''} = n^0_{q''}$, where collision of two phonons, q and q', gives an outgoing phonon q''. When a phonon is excited, the distribution function relaxes to equilibrium as $\Delta n_q(t) = \Delta n_q(t_0)e^{-t/\tau_q}$ in a characteristic time τ_q, which is independent of the rest of the distribution. In other words, the classical RTA assumes that the probability of collisions is independent of the distribution before and after a collision, which is unrealistic. It is usually an approximation for materials having low thermal conductivity and this approach works only when the normal scattering processes dominate over the Umklapp processes.[3,4] It is not a good approximation for high thermal conducting materials such as graphene.

For iterative solution of BTE, the collision term of step *i*+1 is obtained from the previous step *i* in an iterative process. The iterative BTE starts from the RTA relaxation time as a zeroth order solution. In the next step a new relaxation time is calculated from the previous distribution function and the relaxation time. The iterative process is repeated until the convergence is achieved. The iterative method solves the BTE exactly and gives a fully converged value of the lattice thermal conductivity. It is applicable to both low as well as high thermal conducting materials.

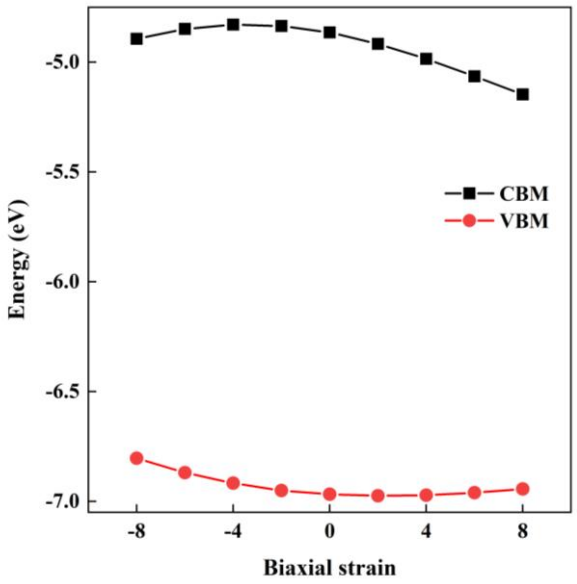

Figure S1. The calculated band alignment of conduction and valence band edges with respect to vacuum under biaxial strain; absolute vacuum is taken as zero.

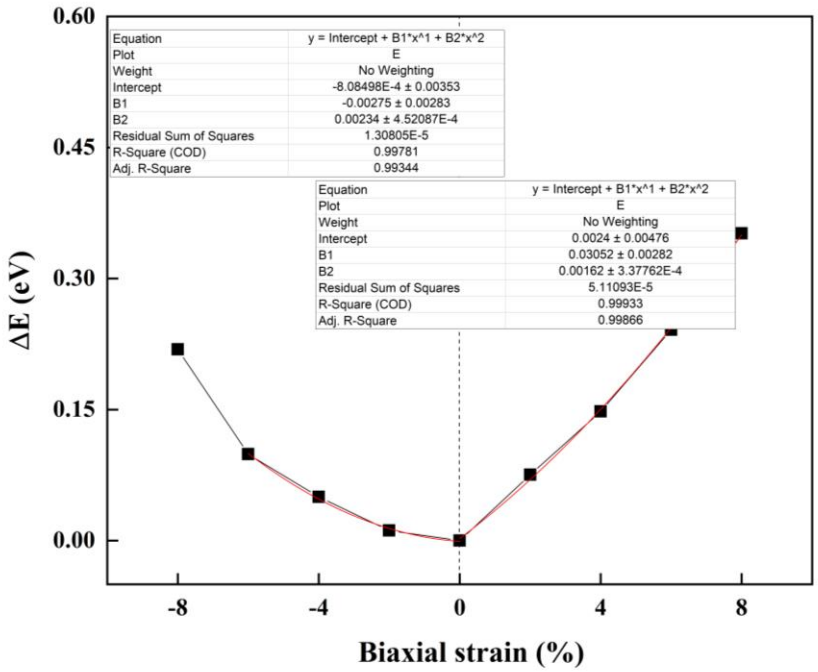

Figure S2. The calculated change in total energy of the system under compressive and tensile biaxial strain

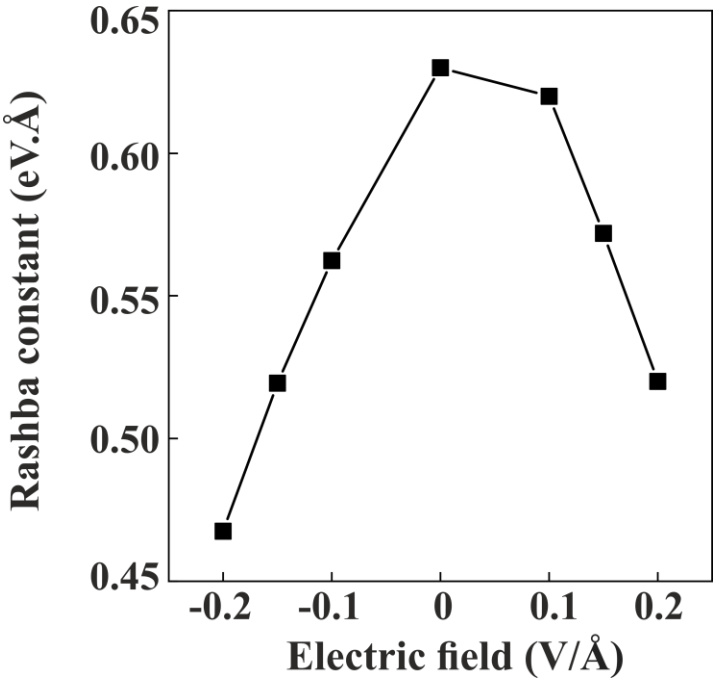

Figure S3: Modulation of Rashba constant under vertical electric field.

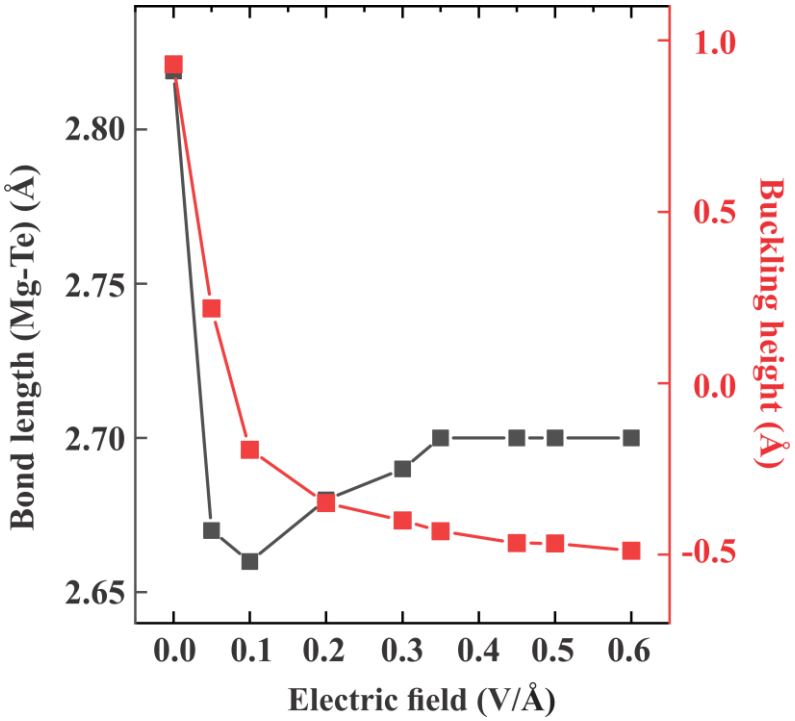

Figure S4. Variation of structural parameters under electric field.

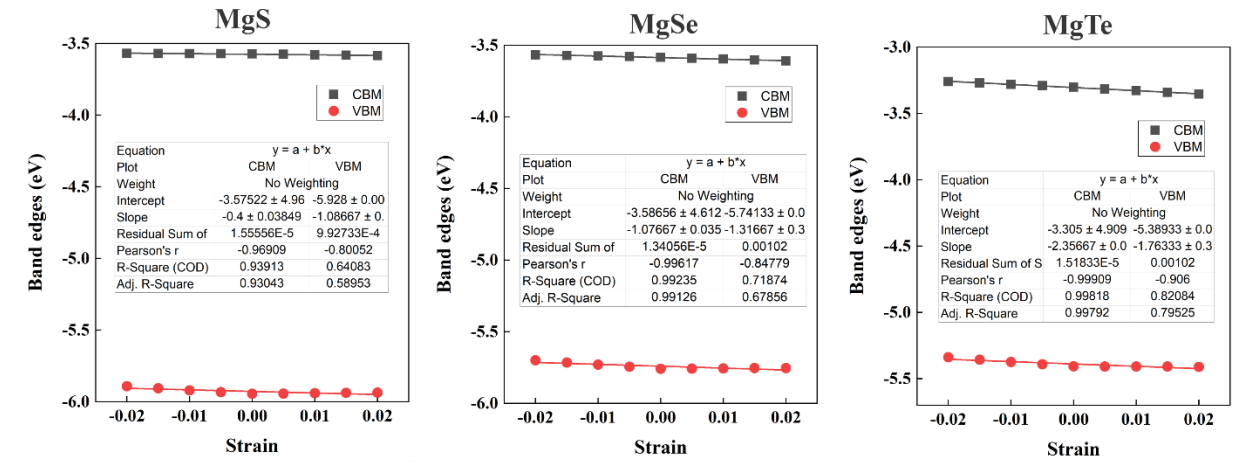

Figure S5: Band edges as a function of small uniaxial strain: slope of CBM (VBM) gives the deformation potential for electrons (holes).

Optical absorbance: The optical properties of material is governed by the characteristics of the electronic band structure. The presence of a finite direct band gap lies in the visible range of the electromagnetic spectra proves that material is optically active. One of the important quantities of optical properties is the absorption coefficient which can be studied using the relation which is a function of the energy[5,6];

$$\alpha_{abs} = \sqrt{2}\omega\left(\sqrt{\left(\varepsilon_1^2(\omega) + \varepsilon_2^2(\omega)\right)} - \varepsilon_1(\omega)\right)^{1/2} \quad \text{(S9)}$$

where $\varepsilon_1(\omega)$ and $\varepsilon_2(\omega)$ are real and imaginary part of complex dielectric function. The optical absorbance spectrum for MgX (X = S, Se, and Te) is provided in Fig. S3. MgTe shows larger absorbance in the visible range due to the small band gap compared to the other two whereas MgS and MgSe are found to be good absorber in the UV range hence MgTe can be used as a visible light photodetector whereas MgS and MgSe can be used as UV-light detector. There is a clear red shift in absorbance spectra due to a decrease in the band gap from MgS to MgTe.

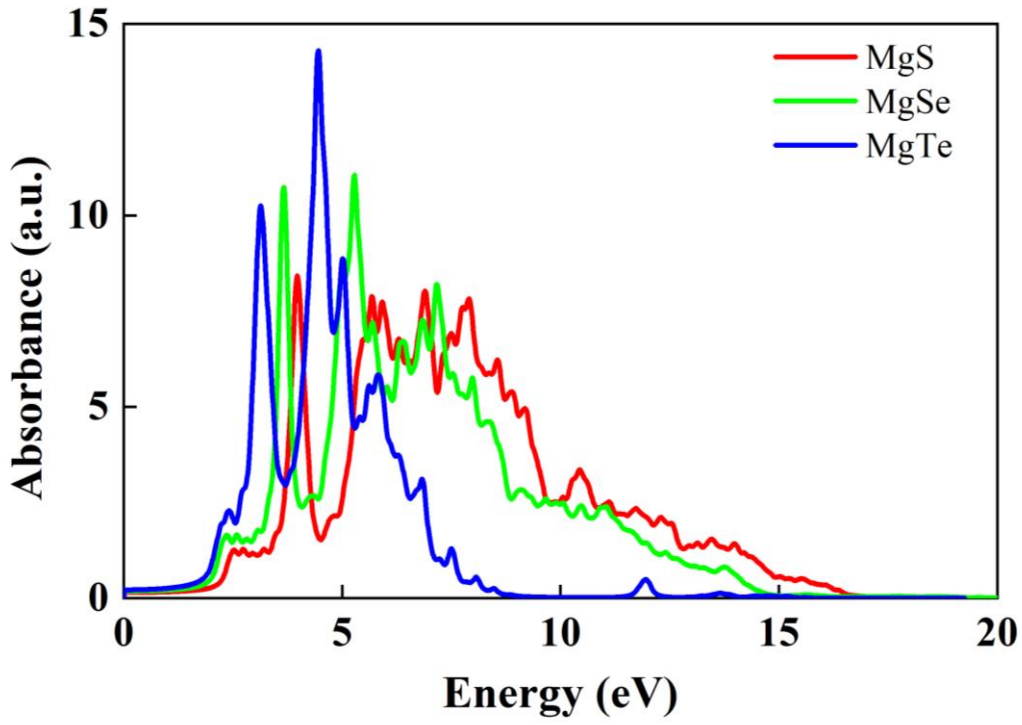

Figure S6. Optical absorbance spectra of MgX (X = S, Se, and Te).

References:

1 R. C. Andrew, R. E. Mapasha, A. M. Ukpong and N. Chetty, *Phys. Rev. B*, 2012, **85**, 125428.
2 P. T. Alvarez, *Thermal transport in semiconductors: first principles and phonon hydrodynamics*, Springer, 2018.
3 B. Peng, H. Zhang, H. Shao, Y. Xu, X. Zhang and H. Zhu, *srep*, 2016, **6**, 20225.
4 A. Shafique, A. Samad and Y.-H. Shin, *Phys. Chem. Chem. Phys.*, 2017, **19**, 20677–20683.
5 A. Rawat, M. K. Mohanta, N. Jena, Dimple, R. Ahammed and A. De Sarkar, *J. Phys. Chem. C*, , DOI:10.1021/acs.jpcc.0c02199.
6 D. Singh, S. K. Gupta, Y. Sonvane and I. Lukačević, *J. Mater. Chem. C*, 2016, **4**, 6386–6390.